Fatigue of an aluminium alloy foam

O. B. Olurin, N. A. Fleck and M. F. Ashby
Cambridge University Engineering Department
Cambridge, CB2 1PZ, UK

Abstract

Tension-tension and compression-compression fatigue tests have been performed on an *Alcan* aluminium alloy foam, in order to determine the stress-life (S-N) behaviour. Under tension-tension loading, the foam progressively lengthens by a plastic strain of about 0.2% due to cyclic ratchetting and to low cycle fatigue of the cell walls, and then the foam fails by the transverse propagation of a dominant tensile crack. In compression-compression fatigue, a crush band is formed and broadens; this leads to the progressive shortening of the specimen by a nominal compressive strain of up to 0.5. The S-N data are best presented in terms of the maximum stress of the fatigue cycle versus fatigue life, where the fatigue life has been defined as the number of cycles for the commencement of progressive shortening in the compression tests and by the number of cycles for material separation in the tension tests.

1 Introduction

Metallic foams show high potential for engineering use, and particularly in multi-functional applications (see for example the recent review by Evans *et al.* [1]). Potential uses of the material are in sandwich structure for panels, tubes and shells, in packaging and crash protection devices, and in heat exchangers. In many of these applications, loading is cyclic compression, and so there exists a need for compression-compression fatigue data. The purpose of the current paper is to characterise the fatigue behaviour of *Alcan*[1] metallic foam under tension-tension and compression-compression cyclic loadings. Alcan foam is produced by bubbling a gas (nitrogen or air) into an aluminium alloy melt and by drawing off the solidified froth. Improved versions of the foam are now produced by *Cymat*[2] under licence to Alcan.

2 Materials under investigation and the experimental procedure

The material studied is an Alcan closed cell aluminium alloy, of average relative density $\bar{\rho}$=0.057, and of designation A356 (7% Si and 0.3% Mg by weight). It comprises a cast aluminium alloy, and the foaming process is stabilised by the presence of 15% SiC distributed randomly within the cell wall [2]. The monotonic properties of the Alcan foam have been measured [3] and are summarised in Table 1. The ultimate tensile strength (σ_{UTS}) is quoted for

---

[1] Supplier: Alcan International Ltd., Box 8400, Kingston Ontario, K7L 5L9, Canada

[2] Cymat address: Cymat Aluminium Corporation, 1245 Aerowood Drive, Mississauga, Ontario L4W 1B9, Canada

tensile tests and the plateau stress, σ_{pl}^{*}, corresponding to a 5% offset plastic strain is quoted for the compressive strength.

Cuboid specimens of dimensions 75 mm x 75 mm x 75 mm were used for compression-compression fatigue tests, while dog-bone specimens of gauge section 50 mm x 50 mm x 55 mm were used for tension-tension fatigue tests. The fatigue tests were performed in both the through-thickness (TT) and in the longitudinal (L) directions for compression-compression loading and in the TT direction for tension-tension loading.

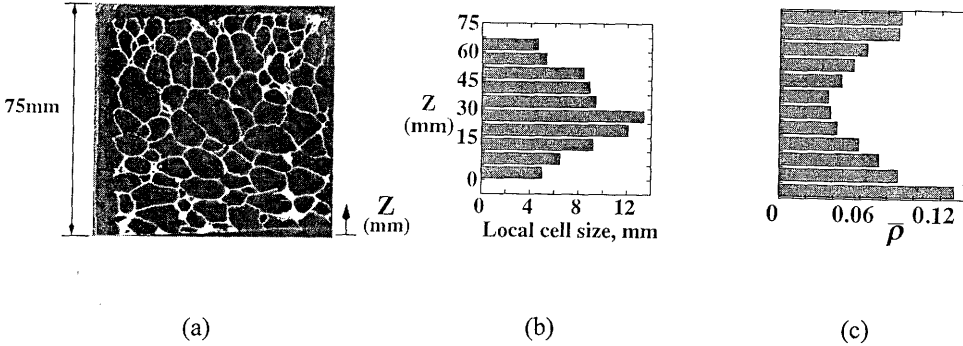(a)   (b)   (c)

Figure 1. (a) Cross-section of Alcan foam; (b) Average cell size against location in TT direction; (c) Relative density $\bar{\rho}$ against location in TT direction.

The Alcan foam shows a strong density variation in the through-thickness direction, with the lowest density at the mid-plane, see Figure 1. This layered structure results in anisotropic mechanical properties: the foam is strongest in the longitudinal (L) direction and is weakest in the through-thickness direction, see Table 1. The fatigue behaviour of the Alcan foam is characterised in terms of its stress versus life, S-N response, under constant amplitude loading. Tests were performed at stress ratios, $R = |\sigma|_{min}/|\sigma|_{max}$ of 0.1 and 0.5 and at a test frequency of 20Hz for both tension-tension and compression-compression loadings. The peak and trough values of the load and displacement were monitored throughout each test.

Table 1: Uniaxial mechanical properties of Alcan metallic foam, of relative density, $\bar{\rho}$=0.057

Loading Direction	Cell size (mm)	Plateau Stress (MPa)	Initial Modulus (GPa)	Nominal densification strain ε_D
L	11.50	1.21	0.17	0.77
T	11.50	0.96	0.11	0.81
TT	11.50	0.25	0.04	0.48

3 Results and Discussion

3.1 Progressive deformation in fatigue

In tension-tension fatigue, the specimens progressively lengthened by a nominal plastic strain of the order of 0.2% before material separation occurred. In contrast, in compression-compression fatigue much larger monotonic plastic strains of the order of 50% gradually developed during the fatigue test. Typical plots of accumulated strain versus the number of cycles for selected stress ranges are shown in Figures 2a and 2b for the Alcan foam of relative density $\bar{\rho}$ = 0.057, under tension-tension and compression-compression loadings, respectively. The figures show the strains measured at the peak and trough values of the loading cycle. For both tension fatigue and compression fatigue, the curves are characterised by an incubation period during which the rate of strain accumulation is negligible (less than 0.1% for tension-tension fatigue, and less than 2% for compression-compression fatigue). In tension-tension cyclic loading, fatigue damage is by the initiation and growth of microcracks in the cell faces, and specimen separation was used to define the fatigue life N_f. A macroscopic crack is generated by the coalescence of many microcracks and leads to specimen separation. The average macroscopic strain in the specimen at separation is of the order of 0.2%, which is an order of magnitude less than the monotonic tensile ductility (about 2%). Optical microscopy at the end of the fatigue tests revealed that only occasional microcracking of cell faces occurs remote from the overall fracture plane.
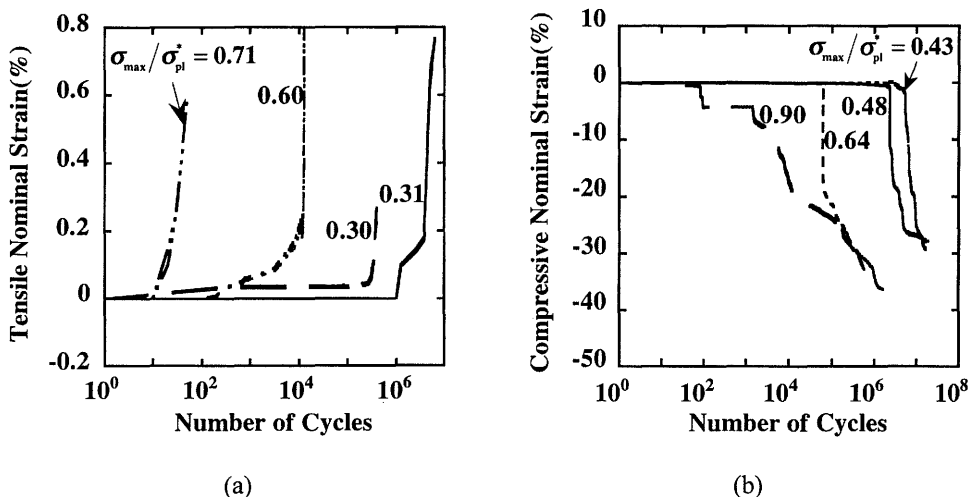

(a) (b)

Figure 2. (a) Progressive lengthening in tension-tension loading of Alcan foam at various stress cycles levels and $R = 0.1$. (b) Shortening of Alcan foam under compression-compression loading at various stress levels. In all the tests $R = 0.1$, and the maximum and minimum strains are shown for each cycle.

In the compression-compression tests the mean component of strain increases in steps until the strain saturates to a fixed level of order 20% to 50% in the compression-compression tests. The saturation of strain level is associated with locking-up of the foam microstructure: opposing cell edges within each cell begin to touch, thereby stiffening and strengthening the foam. The initial knee of the strain versus cycles curve, marking the end of the incubation period is a convenient definition of the fatigue life of the foam, N_f for the compression-compression tests. Progressive strain accumulation is by the sequential collapse of rows of cells. The micrograph in Figure 3

shows a specimen after it has locked-up. A single band is obvious at the centre and the cells around it are still intact and undeformed. Recall that the processing method for the Alcan foam results in a lowest relative density: at the mid-plane, see Figure 1. Consequently, under fatigue loading, the row of cells at the mid-plane collapse first, and then subsequent layers of cells crush later in the fatigue test.

3.2 S-N curves

The fatigue results are conveniently summarised in the form of stress versus life S-N curves by plotting the maximum stress of the fatigue cycle $|\sigma|_{max}$ against the fatigue life N_f. It is convenient to normalise the stress level $|\sigma|_{max}$ by the plateau strength σ_{pl}^* in the monotonic compression tests, and by the ultimate tensile strength $\sigma_{UTS} = \sigma_{pl}^*$ in the tension-tension fatigue tests. σ_{pl}^* and σ_{UTS} are measured on samples from the same foam panel as that used for fatigue tests. As there is some variation of properties [3] from one sample to another, we believe this should account for the observed scatter in stress-life response. In compression-compression fatigue the definition of fatigue life is somewhat arbitrary and we shall use the knee of the curve of strain accumulation versus cycles to define the fatigue life N_f, occurring at a compressive strain of about 2%. The sensitivity of the measured fatigue life to the strain level at which the life is defined is explored in Figure 4a, for compression-compression tests on the Alcan foam at $R = 0.1$, and tested in the TT direction. The curves depict the measured life corresponding to strain levels from 2% (i.e. the knee of the strain-cycles curve) to 30%. We conclude that the fatigue life is sensitive to the assumed strain level for tests performed at high stress level, but the run-out fatigue strength at lives of the order of 10^7 cycles is insensitive to the chosen definition of fatigue life. A fatigue limit was observed for fatigue lives in excess of 10^7 cycles, and we shall define the *endurance ratio* $\sigma_{lim}/\sigma_{pl}^*$ as the value of $|\sigma|_{max}/\sigma_{pl}^*$ at a fatigue life of $N_f = 10^7$ cycles, where N_f is defined by the knee of the strain versus cycles curve.
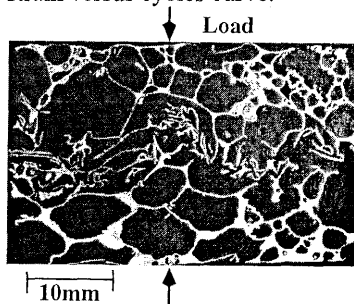

Figure 3. Cross-section of Alcan after lock-up. Compression-compression test performed in the TT direction.

The effect of loading direction (L and TT) upon the compression-compression fatigue response is shown in Figure 4b for $R = 0.1$. Tests were performed in the longitudinal (L) direction, and for this purpose the top and bottom of the foam panels were pre-machined to a depth of 5 mm in order to remove the fully dense skins of the foam prior to testing. Test were also performed on the as-received panels in the through-thickness direction (TT); the transverse direction (T) was not tested because the mechanical properties in the L and T directions were almost identical (see Table 1). We conclude from Figure 4b that the effect of material direction upon the fatigue properties is similar to that noted for the monotonic strength [3]: the difference between the

normalised fatigue strengths in the L and the TT directions of about 20% is small compared with the factor of 5 difference in monotonic strengths. This confirms the usefulness of normalising the fatigue strengths by the monotonic strength in presenting the S-N data.
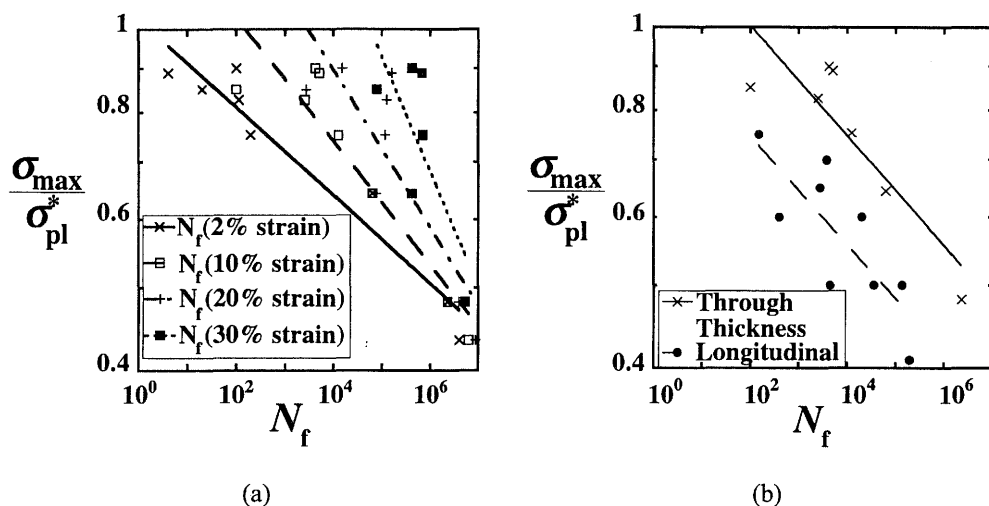

(a)   (b)

Figure 4. (a) S-N curve for cyclic compression of Alcan (TT Direction) at $R = 0.1$. The fatigue life N_f has been defined as the number of cycles to cause a shortening of 2% (i.e. knee of the curve), 10%, 20% or 30%. (b) S-N curve for cyclic compression of Alcan foam in L and TT Directions, with $R = 0.1$.
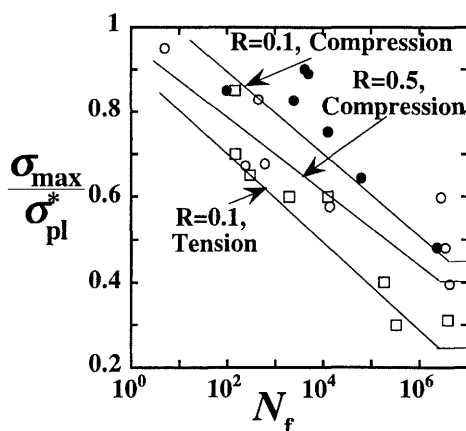

Figure 5.   S-N Curve for cyclic tension and compression of Alcan foam (TT direction) at $R = 0.1$ and 0.5.

S-N curves for compression-compression loading at $R = 0.1$ and 0.5, and for tension-tension loading at $R = 0.1$ are given in Figure 5, for tests in the TT direction. The compression-compression data for $R = 0.1$ and 0.5 coincide to within material scatter. Since the data have been displayed in terms of $|\sigma|_{max}/\sigma_{pl}^*$ rather than as the normalised stress range, we infer that the fatigue life is dominated by the maximum stress of the fatigue cycle. This is not surprising as the failure mode is one of plastic collapse of rows of cells. The tension-tension fatigue curve lies

about 30% below the corresponding compression-compression curve, for $R = 0.1$. The reasonable agreement between tensile and compressive fatigue strengths is consistent with the fact that the so-defined fatigue life is dominated by the fact that the tensile and compressive behaviours are dominated by bending of the cell walls at small macroscopic strains.

For stress levels above the fatigue limit, the fatigue data is well-fitted by the Basquin law,

$$|\sigma|_{max}\, N_f^{\,a} = C \tag{1}$$

where C and the exponent a can be treated as material constants. For the data presented in Figure 5, a is in the range 0.05 to 0.1, in line with the values typically observed for fully dense aluminium alloys [4, 5].
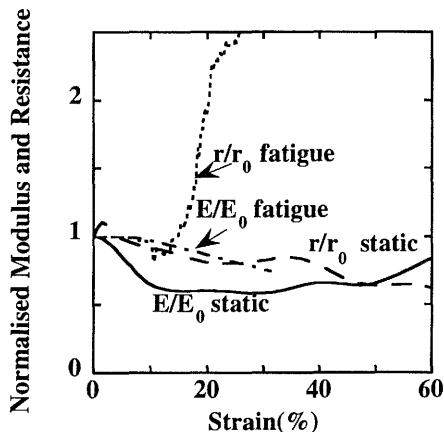

Figure 6. Variation of axial stiffness and electrical resistance with compressive nominal strain for Alcan foam.
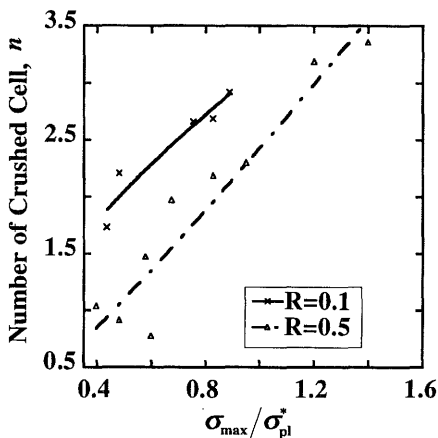

Figure 7. Number of crushed cell after 10^7 cycles, plotted against the maximum stress of the compression-compression loading, for $R = 0.1$ and 0.5.

3.3 Mechanisms of fatigue

In order to determine whether the progressive shortening in compression-compression fatigue is due to the same micromechanisms as in a monotonic test, the unloading modulus normalised by the initial value, E / E_0, and the electrical resistance normalised by the initial value, r / r_0, were monitored during both cyclic and monotonic tests. The unloading modulus in fatigue was measured by measuring the cyclic strain during each fatigue cycle. In a monotonic compression test, the unloading modulus was measured by periodically interrupting the test and unloading the specimen by 10%. The electrical resistance was measured using a DC potential drop technique: a constant current of 3A flowed from the top surface to the bottom surface of the specimen, and the potential difference between the top and bottom of specimen was recorded during the cyclic and monotonic compression tests. Typical results are shown in Figure 6. It is evident that the unloading modulus drops by about 40% and the electrical resistance drops by about 5% when a monotonic compressive strain of 10% is imposed. With a further increase in monotonic strain there is only a small change in the electrical resistance and in the unloading modulus. The initial decrease in electrical resistance and stiffness is associated with the formation of the first crush band (at a monotonic strain of about 10%) with negligible microcracking but with some electrical

contact between cell faces [3]; the change in the cell geometry within the crush band leads to the drop in stiffness. In contrast, in the fatigue test the electrical resistance increases several fold after a strain of 10% has accumulated, due to microcracking of the cell faces . It appears that the electrical resistance method is a promising technique for the detection of fatigue damage within a metallic foam.

The number of crushed layers within the compression-compression fatigue specimens after 10^7 cycles is plotted in Figure 7, for both $R = 0.1$ and 0.5. The total number of cells along the loading direction in each specimen is between 6 and 8. It is clear that the width of the crush band increases with increasing load level. Fatigue failure of the weakest layer of cells at mid-thickness occurs at low cyclic loads, whereas a higher load is required to fail the denser and stronger cells adjacent to the faces of the foam. Thus the number of crushed bands of cells increases with increasing load level.

4 Conclusions

Tension-tension and compression-compression fatigue tests have been performed on Alcan metallic foams. Under tensile fatigue loading, the ductility is small and specimen separation is used to define the fatigue life. In contrast, large plastic strains accumulate in compression-compression fatigue and the fatigue life is defined as the incubation period for the onset of progressive shortening. The main failure mechanism is low cycle fatigue cracking of the cell faces, resulting in a large increase in the electrical resistance of the foam.

References

[1] A. G. Evans, J. W. Hutchinson and M. F. Ashby, Progress in materials Sciences, 43:171-221 (1999).
[2] I. Jin, D. Kenny and H. Sang, U.S. Patent No. 4,973,358 (1990).
[3] O. B. Olurin, N. A. Fleck and M. F. Ashby, Unpublished Research, CUED (1999).
[4] M. F. Ashby and D. R. H. Jones, *Engineering Materials 1*. Butterworth Heinemann, 2nd edition (1996).
[5] R. W. Hertzberg, *Deformation and Fracture Mechanics of Engineering Materials,* John Wiley and Sons, Inc., 4th edition (1996).